HHS Public Access

Author manuscript

Nat Genet. Author manuscript; available in PMC 2017 September 13.

Published in final edited form as:

Nat Genet. 2017 April ; 49(4): 613–617. doi:10.1038/ng.3815.

Germline mutations in *ABL1* cause an autosomal dominant syndrome characterized by congenital heart defects and skeletal malformations

Xia Wang[1,2,11], **Wu-Lin Charng**[1,11], **Chun-An Chen**[1,3,11], **Jill A. Rosenfeld**[1], **Aisha Al Shamsi**[4], **Lihadh Al-Gazali**[5], **Marianne McGuire**[2], **Nicholas Ah Mew**[6], **Georgianne L. Arnold**[7], **Chunjing Qu**[2], **Yan Ding**[8], **Donna M. Muzny**[8], **Richard A. Gibbs**[1,8], **Christine M. Eng**[1,2], **Magdalena Walkiewicz**[1,2], **Fan Xia**[1,2], **Sharon E. Plon**[1,9,10], **James R. Lupski**[1,8,9], **Christian P. Schaaf**[1,3,12,*], and **Yaping Yang**[1,2,12,*]

[1]Department of Molecular and Human Genetics, Baylor College of Medicine, Houston, TX 77030, USA

[2]Baylor Genetics, Houston, TX 77021, USA

[3]Jan and Dan Duncan Neurological Research Institute, Texas Children's Hospital, Houston, TX 77030, USA

[4]Department of Pediatrics, Tawam Hospital, Al-Ain, Abu Dhabi 17172, United Arab Emirates

[5]Department of Pediatrics, College of Medicine & Health Sciences, United Arab Emirates University, Al-Ain, Abu Dhabi 17172, United Arab Emirates

[6]Rare Diseases Institute, Children's National Health System, Washington DC, 20002, USA

[7]Children's Hospital of Pittsburgh of UPMC, Pittsburgh, PA 15224, USA

[8]Human Genome Sequencing Center, Baylor College of Medicine, Houston, TX 77030, USA

[9]Department of Pediatrics, Baylor College of Medicine, Houston, TX 77030, USA

[10]Texas Children's Cancer Center, Texas Children's Hospital, Houston, TX 77030, USA

[*]Correspondence should be addressed to C. P. S. (schaaf@bcm.edu) or Y. Y. (yapingy@bcm.edu).

[11]These authors contributed equally to this work

[12]These authors jointly directed this work

Author Contributions: X.W., Y.Y., W-L.C., C.P.S., C-A.C., and J.R.L. designed the studies. X.W., Y.Y., C.P.S., W-L.C., J.R.L., S.E.P., J.A.R., and F.X. participated in the writing of the manuscript. X.W., C.Q., Y.D., D.M.M., R.A.G, C.M.E, M.W., F.X., and Y.Y. performed sequencing data analysis. W-L.C. and C-A.C. performed the kinase activity assay. X.W., J.A.R., A.A.S., L.A.G., M.M., N.A.M., G.A., C.P.S., and Y.Y. recruited patients and gathered detailed clinical information for the study. Y.Y., C.P.S. and J.R.L. supervised the studies.

Competing Financial Interests: J.R.L. is a paid consultant for Regeneron Pharmaceuticals, holds stock ownership in 23andMe and Lasergen, Inc., is on the scientific advisory board of Baylor Genetics, and is a co-inventor on United States and European patents related to molecular diagnostics. S.E.P. is on the scientific advisory board of Baylor Genetics. The Department of Molecular and Human Genetics at Baylor College of Medicine derives revenue from molecular genetic testing offered at the Baylor Genetics.

URLs: 1000 Genomes, http://browser.1000genomes.org; the Catalogue Of Somatic Mutations In Cancer (COSMIC), http://cancer.sanger.ac.uk/cosmic; ExAC Browser, http://exac.broadinstitute.org/; Ensembl browser, http://www.ensembl.org/index.html; OMIM, http://www.omim.org/; RCSB protein data bank, http://www.rcsb.org/pdb/home/home.do; Uniprot database, http://www.uniprot.org/.

Abstract

ABL1 is a proto-oncogene well known as part of the fusion gene *BCR-ABL* in the Philadelphia chromosome of leukemia cancer cells[1]. Inherited germline *ABL1* changes have not been associated with genetic disorders. Here we report *ABL1* germline variants co-segregating with an autosomal dominant disorder characterized by congenital heart disease, skeletal abnormalities, and failure to thrive. The variant c.734A>G (p.Tyr245Cys) was found as *de novo* or co-segregating with disease in five individuals (families 1-3). Additionally, a *de novo* c.1066G>A (p.Ala356Thr) variant was identified in the sixth individual (family 4). We overexpressed the mutant constructs in HEK 293T cells and observed increased tyrosine phosphorylation, suggesting increased ABL1 kinase activities associated with both p.Tyr245Cys and p.Ala356Thr substitutions. Our clinical and laboratory findings, together with previously reported teratogenic effects of selective BCR-ABL inhibitors in humans[2-5] and developmental defects in *Abl1* knock-out mice[6,7], suggest *ABL1* plays an important role during organismal development.

Somatic and more rarely germline variants leading to activation or mis-expression of proto-oncogenes have long been identified as important cancer drivers. Given the many important functions of proto-oncogenes, it is not surprising that germline variants in these genes can also cause human developmental disorders[8-12].

We identified germline variants in *ABL1* by exome sequencing and Sanger sequencing in six affected individuals who shared similar clinical features including dysmorphic facial features (6/6), congenital heart disease (CHD, 6/6), skeletal abnormalities (6/6), joint problems (5/6), failure to thrive (5/6), gastrointestinal problems (5/6), and male genital/sexual abnormalities (3/4) (Supplementary Table 1 and Supplementary Note). In younger children, dysmorphic features included a broad forehead, small nose, deep-set eyes, and small chin. In older individuals, the face appeared elongated, with a narrow maxilla, long and narrow nose, and pointed chin (Fig. 1A). Common skeletal abnormalities included pectus excavatum, scoliosis, and finger/toe deformities, in particular hindfoot deformity, and finger contractures (Fig. 1B). The CHD included atrial/ventricular septal defects and in older individuals aortic root dilation. Three patients had joint hyper-extensibility/laxity. Most individuals had failure to thrive during infancy and early childhood (Supplementary Fig. 1). Hypospadias/hypogonadism was reported in three of four male patients. Due to cardiac and skeletal manifestations, differential diagnoses commonly included connective tissue disorders, e.g. Marfan syndrome in families 3.

Clinical exome sequencing was performed on the four probands, as previously described (Supplementary Table 2)[13,14]. Exome sequencing and Sanger fill-in of regions poorly covered by exome sequencing did not identify any causal variants in known disease genes (Supplementary Tables 3 and 4). Instead, all probands were found to carry novel heterozygous non-synonymous variants in *ABL1* (NM_007313.2, isoform 1b). One variant, c.734A>G (p.Tyr245Cys), was recurrent in families 1-3, while the other variant, c.1066G>A (p.Ala356Thr), was heterozygous in a single proband from family 4 (Table 1, Figs. 2 and 3 and Supplementary Fig. 2). Sanger sequencing of asymptomatic parents of the probands in families 1 and 2 was negative for p.Tyr245Cys, indicating the variant arose *de novo* in the probands. Subject 1's similarly affected daughter was found to have inherited the

heterozygous p.Tyr245Cys substitution. In family 3, p.Tyr245Cys was found to be inherited from the similarly affected father. In family 4, p.Ala356Thr was found to be *de novo* in the proband.

Unlike many recurrent variants that occur at CpG dinucleotides, the recurrent c.734A>G variant is not located within a CpG site. This variant has been detected in four unrelated but similarly affected individuals (three probands in this report, and a fourth individual who was not included due to lack of consent) from approximately 6,900 consecutive and unrelated individuals referred for clinical exome sequencing. There is significant enrichment of this variant in our affected patient cohort compared to 0/60700 in the database from Exome Aggregation Consortium (ExAC, accessed July 2016, P value $<1\times10^{-8}$, Supplementary Data 1).

ABL1 has two isoforms, 1a (NM_005157.5) and 1b (NM_007313.2), as a result of an alternatively spliced first exon. Isoform 1b has 19 additional N-terminal residues that are absent in isoform 1a; myristoylation of these residues plays a role in autoinhibition of the kinase activity. The two missense variants in our patients are expected to affect both isoforms. Residues p.Tyr245 and p.Ala356 in isoform 1b correspond to p.Tyr226 and p.Ala337 in isoform 1a, respectively.

In order to investigate the potential effects of the two *ABL1* variants, we transiently transfected HEK 293T cells with C-terminally tagged wild-type and mutant plasmid constructs using cDNA of both human *ABL1* isoforms (Fig. 4 and Supplementary Figs. 3-5). Endogenous levels of overall phosphotyrosine (p-Tyr) and phosphorylation of specific ABL1 substrates (STAT5) were measured by immunoblotting. Overexpression of the mutant constructs in both isoforms resulted in increased overall phosphotyrosine (p-Tyr) and increased phosphorylation of specific ABL1 substrates (STAT5) when compared to wild-type (Fig. 4 and Supplementary Fig. 5). These results indicate that both the c.734A>G (p.Tyr245Cys) and c.1066G>A (p.Ala356Thr) variants cause increased phosphorylation suggesting increased ABL1 kinase activity.

Of note, p.Tyr245 and p.Ala356 are both known as key residues regulating ABL1 kinase activity. The p.Tyr245 residue is one of the two tyrosine residues required for autophosphorylation-induced activation of ABL1 intrinsic kinase activity. It was shown that while autophosphorylation causes an 18-fold increase in the activity of wild-type ABL1, introduction of p.Tyr245Phe, which affects the same residue as p.Tyr245Cys in families 1-3, results in inhibition of such activation by 50%[15]. This is in contrast to the increased phosphorylation associated with the p.Tyr245Cys substitution in this study. To exclude the possibility of systematic differences between our experimental settings and those reported previously[15], we overexpressed the reported mutant construct. Consistent with the previous report, we observed decreased overall phosphotyrosine (p-Tyr) for p.Tyr245Phe when compared to the wild-type in both isoforms (Supplementary Figs.6 and 7). These results support the contention that the p.Tyr245Phe and p.Tyr245Cys substitutions have opposite effects (gain-of-function vs. loss of function) on ABL1 kinase activities.

The p.Ala356 residue is located in the myristoyl-binding site of the ABL1 kinase domain which intra molecularly binds the N-terminal myristoyl group and forms an autoinhibition conformation. It was shown that p.Ala356Asn, which affects the same amino acid as p.Ala356Thr identified in family 4, resulted in higher kinase activity than wild-type[16]. Our findings on the p.Ala356Thr mutant suggest that these two changes affecting p.Ala356, i.e. to Asn versus to Thr, have similar effects. Of note, residue p.Ala356 in isoform 1b is located in the binding site for the N-terminal myristoyl group, which is unique to isoform 1b. However, our data showed that the substitution of this residue in isoform 1a, p.Ala337Thr, also caused increased phosphorylation (Supplementary Fig. 5).

To test whether mutant *ABL1* transcript is expressed in the affected individuals, we conducted semi-quantitative RT-PCR on lymphoblast-derived cell lines from affected subjects 1 and 2 (F1:II1 and F1:III1), and an unaffected control (F1:II2) (cell lines from other individuals not available). Sanger sequencing of the RT-PCR products showed approximate 1:1 ratios of *ABL1* wild-type and mutant alleles (Supplementary Fig. 8), indicating similar levels of *ABL1* expression in affected and control.

Mouse models suggest an important role of *ABL1* during development. *Abl1* knockout mice have growth delay, cardiac hyperplasia and osteoporosis[6,7]. We re-evaluated the ventricular wall thickness of our patients and confirmed that there is no cardiac hyperplasia (data not shown). This may be due to that variants identified in this study lead to increased phosphorylation while the mice have *Abl1* null alleles. Overexpression of wild-type *Abl1*, but not kinase defective *Abl1*, can rescue the mutant phenotypes of *Abl1* knockout mice, suggesting that ABL1 kinase activity is essential for normal development[17].

Intriguingly, severe congenital malformations have been reported in fetuses exposed to imatinib, a selective tyrosine kinase inhibitor drug, which inhibits BCR-ABL, c-KIT, and PDGFRA, used in the treatment of multiple cancers, most notably Philadelphia-chromosome (BCR-ABL) positive CML, raising concern for potential teratogenic effects of the drug[2-5]. Pye et al. studied a cohort of 180 women exposed to imatinib during pregnancy, and identified 12 fetuses with abnormalities, most of which were exposed to the drug during the first trimester. Anomalies of the 12 fetuses included scoliosis/vertebral defects (3), CHD (2), hypospadias (2), and pyloric stenosis (1)[2,3]. Based on the small number of cases, no definitive conclusions about the potential teratogenicity of imatinib can be drawn, especially as some of the cases were also exposed to additional teratogens, such as Coumadin/warfarin or hydroxyurea. Others have reported potential teratogenic effects of imatinib, including CHD, skeletal anomalies, hypospadias, intestinal malrotation, and imperforate anus[4,5]. This spectrum of phenotypes overlaps with what was found in our patients, including scoliosis (3/6), CHD (6/6), hypospadias/hypogonadism (3/4), pyloric muscle thickening (1/6), and imperforate anus (1/6). These similarities between fetuses exposed to imatinib during pregnancy and human patients with constitutional *ABL1* variants, along with the studies in mice, suggest that ABL1 function needs to be tightly regulated during development, and dysregulation can cause congenital malformations.

Our data suggest a novel genetic syndrome caused by constitutional *ABL1* variants, which affects growth, and the cardiovascular and skeletal systems. The differential diagnosis of the

newly described syndrome includes Shprintzen-Goldberg syndrome (dolichostenomelia, arachnodactyly, pectus deformity, scoliosis, aortic root enlargement, and high-arched palate) and Loeys-Dietz syndrome (long face, high-arched palate, microretrognathia, pectus deformity, scoliosis, arachnodactyly, joint laxity, and aortic root aneurysm with risk of dissection). Given the evidence of increased transforming growth factor-beta (TGF-β) signaling associated with connective tissue disorders, we investigated whether *ABL1* variants affect TGF-β signaling by measuring the phosphorylation level of SMAD2 and SMAD3. In the context of our experimental settings, we did not observe significant alteration in the phosphorylation level of SMAD2 and SMAD3 (Fig. 4 and Supplementary Figs. 4 and 5).

Malignancies have not been detected in any of the affected individuals with *ABL1* germline variants, but as they cause increased phosphorylation and possibly increased kinase activity of this proto-oncogene, it may be prudent to perform systematic clinical screening for *ABL1*-associated cancers in the newly identified individuals.

In conclusion, we report that germline variants in *ABL1* cause a syndrome characterized by congenital heart disease, skeletal abnormalities, and failure to thrive. *ABL1* joins the growing list of genes that are implicated in both cancer and human developmental disorders.

Online Methods

Research Subjects

Written informed consent for all subjects was obtained in accordance with protocols approved by the appropriate human subject ethics committees at Baylor College of Medicine and United Arab Emirates University.

Exome Sequencing

Exome sequencing was performed as previously described[13,14]. Briefly, genomic DNA samples were fragmented, ligated to Illumina multiplexing paired-end adapters, amplified with indexes added, and hybridized to a solution based exome capture reagent (Roche NimbleGen). Paired-end sequencing (100 bp × 2) was performed on Illumina HiSeq 2500 platform to provide a mean sequence coverage of about 120×, with about 97% of the target bases having at least 20× coverage (Supplementary Table 2).

Sequencing Data Analysis and Annotation

Exome sequencing data was processed and the variants were annotated as previously described[13,14]. Briefly, the output data from the Illumina HiSeq 2500 were converted from a bcl file to a FastQ file by Illumina Consensus Assessment of Sequence and Variation software version 1.8.3, and mapped to the human-genome reference using BWA program[23]. Variants were called by Atlas-SNP and Atlas-indel[24]. An in-house software program, CASSANDRA, was used for variant filtering and annotation[13].

cDNA Constructs

ABL1 1b isoform cDNA clone (MHS6278-211687872) was purchased from GE Dharmacon (MGC cDNA collection). *ABL1* 1a isoform cDNA was obtained by PCR of the 1b isoform cDNA using *ABL1* 1a isoform specific primers. All point mutations were generated by QuikChange site-directed mutagenesis kit (Agilent). All constructs were verified by Sanger sequencing (Supplementary Fig. 3).

Wild-type and mutant human *ABL1* cDNA constructs were cloned into pcDNA™3.1/V5-His A (with C-terminal V5 and His tags; Clontech) using KpnI and XhoI restriction enzyme sites. Residues p.Tyr245 and p.Ala356 in isoform 1b correspond to p.Tyr226 and p.Ala337 in isoform 1a, respectively. Restriction enzymes are from NEB, and DNA purification kits are from Invitrogen and Qiagen.

Cell Culture and Western Blot

HEK 293T cell line was cultured in Dulbecco's Modified Eagle Medium (Corning 45000-312) with 10% fetal bovine serum, L-glutamine, and antibiotics-antimycotics at 37 °C under 5% CO_2. The transfection was performed using Lipofectamine 2000 (ThermoFisher Scientific) according to the manufacturer's instructions. Cells were harvested 24 hrs after transfection. Cells were lysed in lysis buffer [50 mM Tris-HCl pH 7.5, 150 mM NaCl, 5% glycerol, 0.5% TritonX-100, protease inhibitor cocktail and phosphatase inhibitor Xpert (Gendepot)]. The lysate supernatant was boiled in Laemmli buffer. Polyacrylamide gel electrophoresis, transfer, and Western blot were performed according to standard protocols. Primary antibodies were used at the following dilution: mouse α-c-Abl 1:100 (EMD Millipore OP-20), mouse α-pTyr 4G10 1:20,000 (EMD Millipore 05-321), PathScan bcr/abl antibody mixture 1:400 (Cell signaling 5300S), mouse α-V5 1:10,000 (ThermoFisher Scientific 460705), mouse α-GAPDH 1:20,000 (Advanced ImmunoChemical, 2-RGM2), and rabbit α-pSmad2/3 1:1,000 (Cell signaling 8828S). Goat anti rabbit HRP-conjugated secondary antibody (Bio-rad 170-5046) was used at 1:10,000, and Donkey anti mouse HRP-conjugated secondary antibody (Jackson ImmunoResearch 715-035-150) was used at 1:10,000.

The Western blot analysis was performed in three technical replicates from separate transfections of the same cell culture. The P values were calculated using one-way ANOVA with Tukey's post hoc analysis. The exact numbers used for the calculation are provided in the Supplementary Data 1. The experiment shown was replicated three times in the laboratory.

Semi-quantitative RT-PCR on lymphoblast cell lines

Total RNA was extracted from human lymphoblast cell lines from subjects 1, 2, and the control with the miRNeasy Mini Kit (Qiagen) following manufacturer's instructions. RNA was quantified by NanoDrop 1000 (Thermo Fisher). 3 ug of total RNA was reverse transcribed to cDNA by the reverse transcription kit (Qiagen). cDNA from each sample were then analyzed by RT-PCR followed by Sanger sequencing. Semi-quantitative PCR cycle number: *ABL1* (exon 3-exon 5) 35 cycles; *ABL1* (exon 3-exon 6) 35 cycles; *GAPDH* 25 cycles. PCR primer sequences are available in Supplementary Table 5.

Data availability

The c.734A>G (p.Tyr245Cys) and c.1066G>A (p.Ala356Thr) variant has been submitted to the ClinVar database (https://www.ncbi.nlm.nih.gov/clinvar/) with accession code SCV000485092 and SCV000485097, respectively. The raw whole-exome sequencing data that support the findings of this study are available on request from the corresponding author (Y.Y.) and are not publicly available due to them containing information that could compromise research participant privacy. All other data generated or analyzed during this study are included in this published article (and its supplementary information files).

Supplementary Material

Refer to Web version on PubMed Central for supplementary material.

Acknowledgments

We thank the families for their participation and collaboration. This work was funded in part by the US National Human Genome Research Institute (NHGRI)/National Heart Lung and Blood Institute (NHLBI) grant number U54HG006542 to the Baylor-Hopkins Center for Mendelian Genomics (BH-CMG) and the NIH Common Fund, through the Office of Strategic Coordination/Office of the NIH Director under Award Number U01HG007709. W-L.C. was supported by Cancer Prevention Research Institute of Texas (CPRIT) training Program RP140102. N.A.M.'s work is supported by the Rashid Family Fund.

References

1. de Klein A, et al. A cellular oncogene is translocated to the Philadelphia chromosome in chronic myelocytic leukaemia. Nature. 1982; 300:765–7. [PubMed: 6960256]
2. Pye SM, et al. The effects of imatinib on pregnancy outcome. Blood. 2008; 111:5505–8. [PubMed: 18322153]
3. Apperley J. Issues of imatinib and pregnancy outcome. J Natl Compr Canc Netw. 2009; 7:1050–8. [PubMed: 19930974]
4. Jain N, Sharma D, Agrawal R, Jain A. A newborn with teratogenic effect of imatinib mesylate: a very rare case report. Med Princ Pract. 2015; 24:291–3. [PubMed: 25896670]
5. Ault P, et al. Pregnancy among patients with chronic myeloid leukemia treated with imatinib. J Clin Oncol. 2006; 24:1204–8. [PubMed: 16446320]
6. Li B, et al. Mice deficient in Abl are osteoporotic and have defects in osteoblast maturation. Nat Genet. 2000; 24:304–8. [PubMed: 10700189]
7. Qiu Z, Cang Y, Goff SP. c-Abl tyrosine kinase regulates cardiac growth and development. Proc Natl Acad Sci U S A. 2010; 107:1136–41. [PubMed: 20080568]
8. Tartaglia M, et al. Mutations in PTPN11, encoding the protein tyrosine phosphatase SHP-2, cause Noonan syndrome. Nat Genet. 2001; 29:465–8. [PubMed: 11704759]
9. Yang W, et al. Ptpn11 deletion in a novel progenitor causes metachondromatosis by inducing hedgehog signalling. Nature. 2013; 499:491–5. [PubMed: 23863940]
10. Hafner C, Toll A, Real FX. HRAS mutation mosaicism causing urothelial cancer and epidermal nevus. N Engl J Med. 2011; 365:1940–2. [PubMed: 22087699]
11. Aoki Y, et al. Germline mutations in HRAS proto-oncogene cause Costello syndrome. Nat Genet. 2005; 37:1038–40. [PubMed: 16170316]
12. Lahiry P, Torkamani A, Schork NJ, Hegele RA. Kinase mutations in human disease: interpreting genotype-phenotype relationships. Nat Rev Genet. 2010; 11:60–74. [PubMed: 20019687]
13. Yang Y, et al. Clinical whole-exome sequencing for the diagnosis of mendelian disorders. N Engl J Med. 2013; 369:1502–11. [PubMed: 24088041]
14. Yang Y, et al. Molecular findings among patients referred for clinical whole-exome sequencing. JAMA. 2014; 312:1870–9. [PubMed: 25326635]

15. Brasher BB, Van Etten RA. c-Abl has high intrinsic tyrosine kinase activity that is stimulated by mutation of the Src homology 3 domain and by autophosphorylation at two distinct regulatory tyrosines. J Biol Chem. 2000; 275:35631–7. [PubMed: 10964922]
16. Hantschel O, et al. A myristoyl/phosphotyrosine switch regulates c-Abl. Cell. 2003; 112:845–57. [PubMed: 12654250]
17. Hardin JD, Boast S, Mendelsohn M, de los Santos K, Goff SP. Transgenes encoding both type I and type IV c-abl proteins rescue the lethality of c-abl mutant mice. Oncogene. 1996; 12:2669–77. [PubMed: 8700526]
18. Nagar B, et al. Structural basis for the autoinhibition of c-Abl tyrosine kinase. Cell. 2003; 112:859–71. [PubMed: 12654251]
19. Guex N, Peitsch MC. SWISS-MODEL and the Swiss-PdbViewer: an environment for comparative protein modeling. Electrophoresis. 1997; 18:2714–23. [PubMed: 9504803]
20. Kumar P, Henikoff S, Ng PC. Predicting the effects of coding non-synonymous variants on protein function using the SIFT algorithm. Nat Protoc. 2009; 4:1073–81. [PubMed: 19561590]
21. Adzhubei IA, et al. A method and server for predicting damaging missense mutations. Nat Methods. 2010; 7:248–9. [PubMed: 20354512]
22. Schwarz JM, Cooper DN, Schuelke M, Seelow D. MutationTaster2: mutation prediction for the deep-sequencing age. Nat Methods. 2014; 11:361–2. [PubMed: 24681721]
23. Li H, Durbin R. Fast and accurate long-read alignment with Burrows-Wheeler transform. Bioinformatics. 2010; 26:589–95. [PubMed: 20080505]
24. Shen Y, et al. A SNP discovery method to assess variant allele probability from next-generation resequencing data. Genome Res. 2010; 20:273–80. [PubMed: 20019143]

Figure 1.

The facial and skeletal features of subjects 1 (F1:II1), 2 (F1:III1), 3 (F2:II1), and 6 (F4:II1). (A) Facial features. From left to right: subjects 1, 2, 3, and 6. Note long face with narrow maxilla and pointed chin in subjects 1 and 3. Younger individuals (subjects 2 and 6) manifest broad forehead, deep-set eyes, small nose, and small chin. (B) Skeletal abnormalities. From left to right: subjects 1, 2, 3, and 6. Pectus excavatum, scoliosis, hindfoot deformity, causing pes planus, and finger contractures.

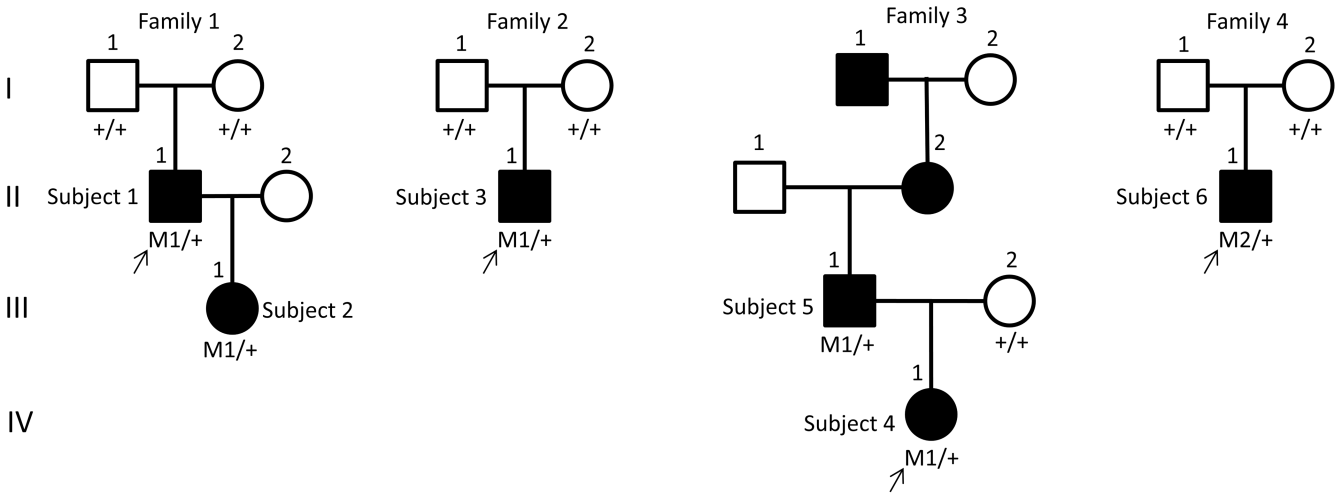

M1: c.734A>G (p.Tyr245Cys)

M2: c.1066G>A (p.Ala356Thr)

Figure 2.

Identification of *ABL1* variants in affected families. The pedigrees of the four families. The genotypes are shown below each individual in the pedigrees with "+" representing the reference allele and "M" representing the mutant allele. Individuals without genotype symbols do not have samples available for genotyping.

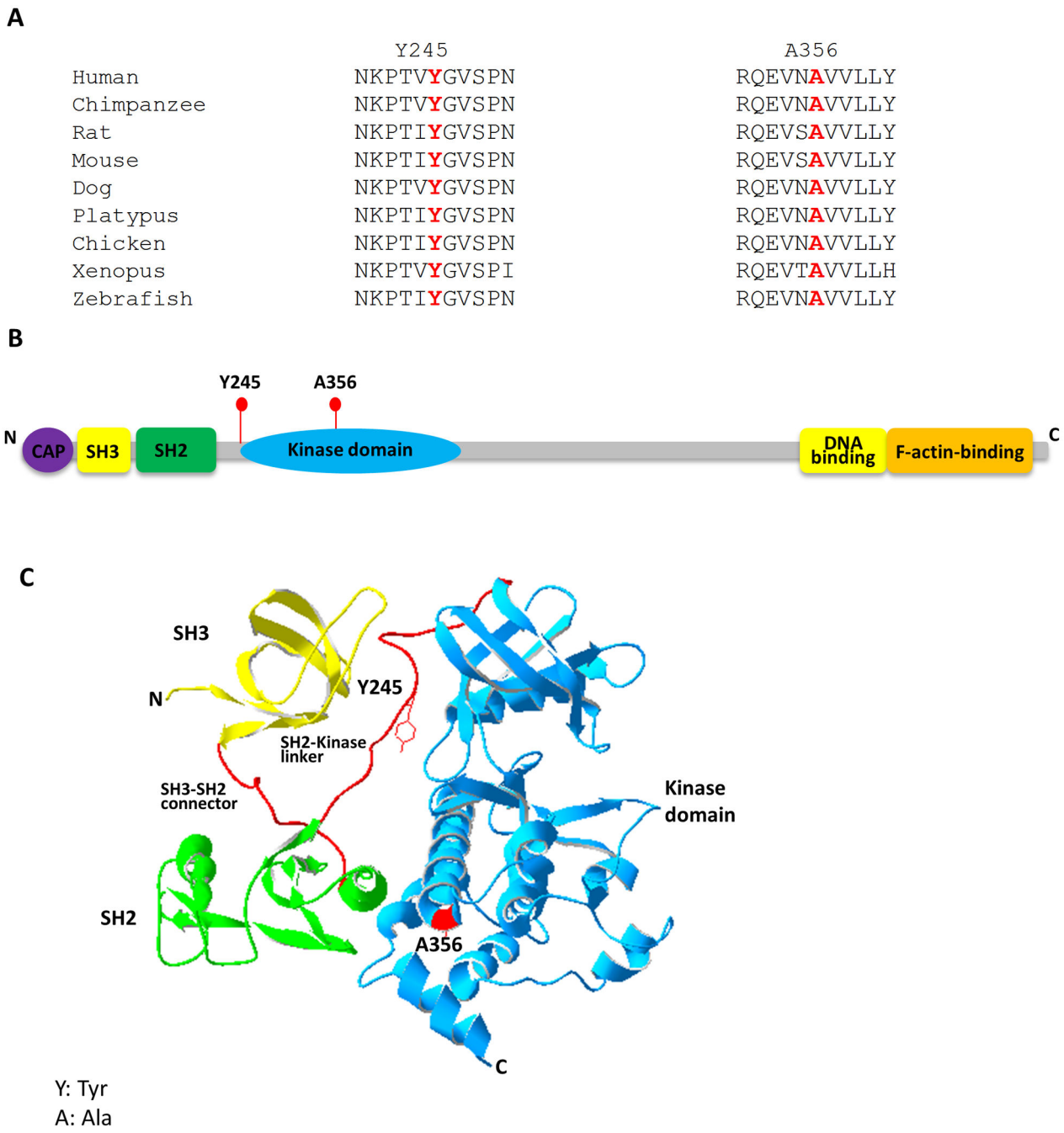

Figure 3.

In silico analysis of the two *ABL1* variants identified in this study. (A) The Tyr245 and Ala356 residues are conserved from human to zebrafish (prepared based on Ensembl browser genomic alignments). (B) The schematic view of ABL1 1b protein isoform and its domains. The Tyr245 residue localizes in the linker region between the SH2 and kinase domains, while the Ala356 localizes in the kinase domain. Prepared based on UniProt database domains, ID P00519. (C) The 3D structure of ABL1 1b protein isoform, its N-

terminal domains, and the localization of the two mutated *ABL1* residues. Based on the structural data from Nagar et al., 2003 (PDB ID 1OPL)[18] using Swiss-PdbViewer[19].

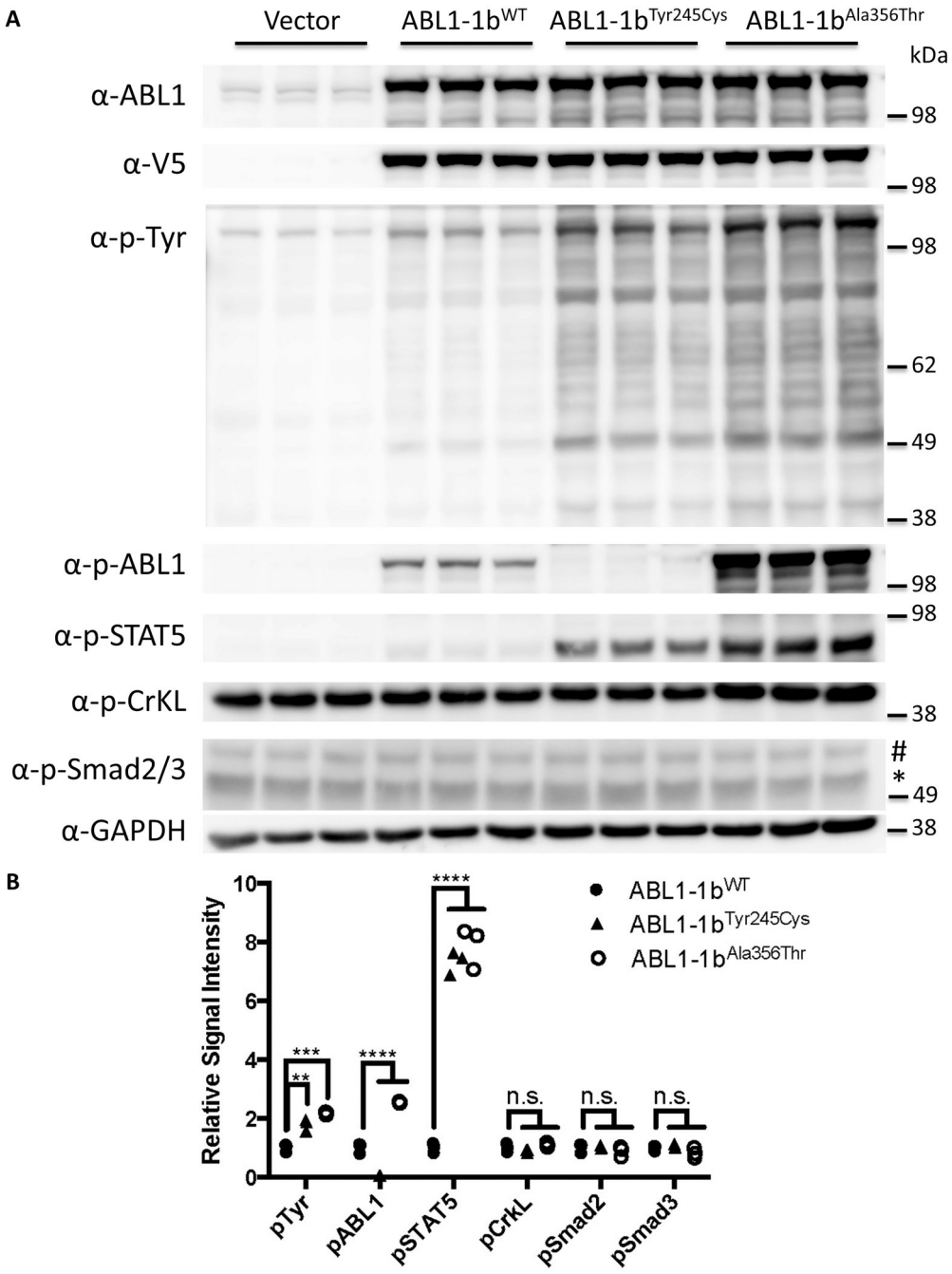

Figure 4.

The effect of *ABL1* variants (isoform 1b) on phosphorylation. (A) Overall phosphotyrosine levels and phosphorylation of specific ABL1 substrates were analyzed by transiently expressing the wildtype and mutant constructs in HEK 293T cells and immunoblotting. Both variants showed increased overall phosphotyrosine levels and phosphorylation of STAT5 when compared with wild-type. Increased phosphorylated ABL1 was observed for Ala356Thr but not Tyr245Cys due to the substitution of the Tyr245 residue, which is recognized by the anti-phospho-ABL1 antibody. No significant difference in the

phosphorylation levels of CrKL, SMAD2 and SMAD3 between mutants and wild-type were observed. Antibodies used in the detection include anti-phosphotyrosine (p-Tyr) for the overall phosphotyrosine level, anti-phospho-ABL1 (p-ABL1), anti-phospho-STAT5 (p-STAT5), anti-phospho-CrkL (p-CrkL), and anti-phospho-SMAD2 and SMAD3 (p-Smad2/3) antibodies for the phosphorylation level of specific ABL1 substrates in the whole cell lysates. The level of GAPDH is used as an internal loading control. Experiments for each construct were performed in triplicates. Pound and asterisk symbols in the panel A denote p-Smad2 and p-Smad3 respectively. (B) Quantification of the Western blot results. Data are normalized to GAPDH protein levels, with the wild-type set at 1.0. **: $P \leq 0.01$; ***: $P \leq 0.001$; ****: $P \leq 0.0001$; n.s.: $P > 0.05$.

Nat Genet. Author manuscript; available in PMC 2017 September 13.

Table 1

Summary of *ABL1* variants identified in the subjects

Family	Coordinate (hg19)/Location	Nucleotide change/ Amino acid change [a]	*In Silico* Predictions[20-22]	NGS reads in proband (mutant : normal)	Inheritance	Functional consequences in this study	Previous functional studies on residues p.Try245 and p.Ala356
1	Chr9: 133738277 Exon 4	c.734A>G (p.Tyr245Cys)	Damaging by SIFT; Probably damaging by PolyPhen2; Disease causing by MutationTaster	75:69	*De novo* in proband, transmitted to affected daughter	Increase tyrosine phosphorylation	Tyrosine to phenylalanine at the same p.Try245 residue leads to inhibition of autophosphorylation-induced activation of ABL1 intrinsic kinase activity[15]
2				82:71	*De novo* in proband		
3				310:255	Proband inherited the variant from affected father		
4	Chr9: 133748348 Exon 6	c.1066G>A (p.Ala356Thr)	Damaging by SIFT; Probably damaging by PolyPhen2; Disease cause by MutationTaster	46:68	*De novo* in proband	Increase tyrosine phosphorylation	Alanine to asparagine at the same p.Ala356 residue leads to higher ABL1 kinase activity[16]

[a] Genbank transcript ID used for the nucleotide and amino acid change in isoform 1b: NM_007313.2

The two variants above are absent in the dbSNP, ESP, ExAC, and COSMIC databases.